Proceedings of the 2000 IEEE
International Conference on Robotics & Automation
Seoul, Korea • May 21-26, 2001

Design of Continuous Alternate Wheels for Omnidirectional Mobile Robots

Kyung-Seok Byun, Sung-Jae Kim, Jae-Bok Song

Department of Mechanical Engineering, Korea University
5-ga Anam-dong Sungbuk-gu, Seoul, 136-701, Korea.
E-mail: jbsong@korea.ac.kr

Abstract

Many types of omnidirectional wheels with passive rollers have a gap between rollers. This gap causing the wheel to make discontinuous contact with the ground, leads to vertical and/or horizontal vibrations. In this paper a novel design of continuous alternate wheel was proposed to minimize a gap between rollers. In the continuous alternate wheel, inner and outer rollers are arranged continuously, thus resulting in no gap between the rollers. This paper details the design process including the systematic approaches to determine the optimum number of rollers, the radii of rollers and the inclination angle of the inside of an outer roller for given design specifications. Finally, an actual continuous alternate wheel is constructed to verify validity of the design guidelines.

1. Introduction

Applications of wheeled mobile robots have recently extended to service robots for the handicapped or the aged and industrial mobile robots working in various environments. The most popular wheeled mobile robot is equipped two independent driving wheels. This robot can rotate about any point, but does not allow sideways motion. To overcome this drawback, mobile robots with steerable wheels were suggested. They allow both rotation and sideways motions but not simultaneously. If such robots are used as service robots, for example, they may get in the way of a person they assists, require unnecessarily large space or move along a complicated path when changing their direction.

To cope with these problems, omnidirectional mobile robots have been proposed. They are capable of arbitrary motion in an arbitrary direction without changing the direction of wheels, because they can achieve 3 DOF motion on a two-dimensional plane. Various types of omnidirectional mobile robots have been proposed so far; off-centered wheels [1], ball wheels [2], and universal wheels [3] are more popular among them.

The initial universal wheel design shown in Fig. 1a has multiple passive rollers whose axes are positioned tangent to the wheel circumference. Since this type of wheel makes discontinuous contact with the ground due to a gap between successive rollers, however, the robot platform suffers form vertical vibrations. To minimize the gap between rollers, various variations of universal wheels have been devised. In the Mecanum wheel [4] shown in Fig. 1b, rollers are arranged in such a way that the contact between the wheel and the floor is continuous. In the double wheels [5] shown in Fig. 1c, wheels are arranged in an overlapping way. These types of wheels touch the ground continuously, but the points of contact with the ground are not continuous as seen in the figure. This discontinuous contact causes horizontal vibrations [6].

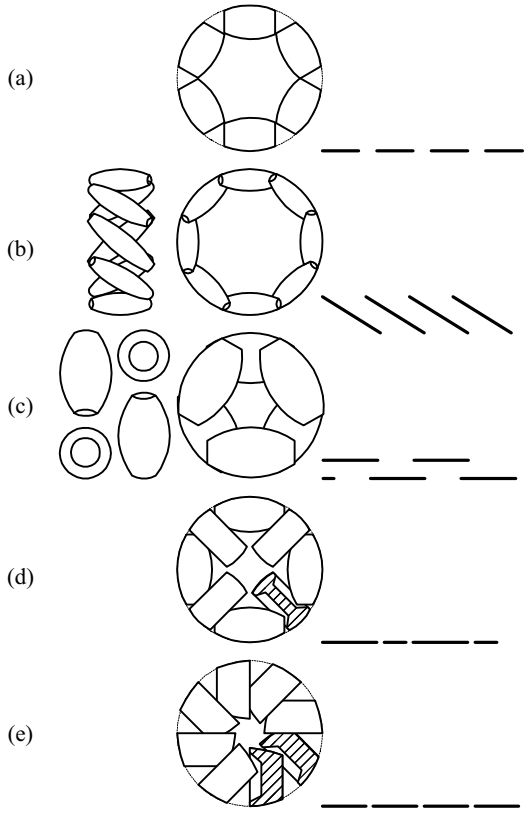

Fig. 1 Various wheel types using passive rollers and their traces; (a) classic, (b) Mecanum, (c) double, (d) alternate, and (e) half.

Other attempts have been made to minimize the gap between rollers for reduction in horizontal and vertical vibrations. In the alternate wheel mechanism [7] shown in Fig. 1d, the large and small rollers are alternated to reduce the gap size. In the half wheel mechanism [6] shown in Fig. 1e, half-divided rollers are arranged in an overlapping manner. However, the gap between rollers cannot be eliminated completely even in these wheels.

In this research a new type of universal wheel is proposed to cope with the problems caused by the gap between the rollers. This new wheel features virtually no gap between passive rollers. Because this wheel makes continuous contact with the ground and has alternating large and small rollers about the wheel, this wheel will be termed a continuous alternate wheel (CAW).

0-7803-6475-9/01/$10.00© 2001 IEEE

This paper presents details in the design procedure and construction of the continuous alternate wheel. Chapter 2 provides the detailed design in the number of rollers and the shape and size of rollers. Chapter 3 is concerned with the overall structure of a continuous alternate wheel. Finally, conclusions are drawn and future work is outlined in Chap.4.

2. Design of passive rollers

The rollers used in a universal wheel are barrel-shaped as shown in Fig. 2, because the surface contour of a roller should match the wheel circumference. Fig. 2 shows a universal wheel with smaller inner rollers and larger outer rollers arranged alternately around it. In each roller, the most convex radius in the middle is termed a maximum radius, and the radius at its ends is termed a minimum radius.

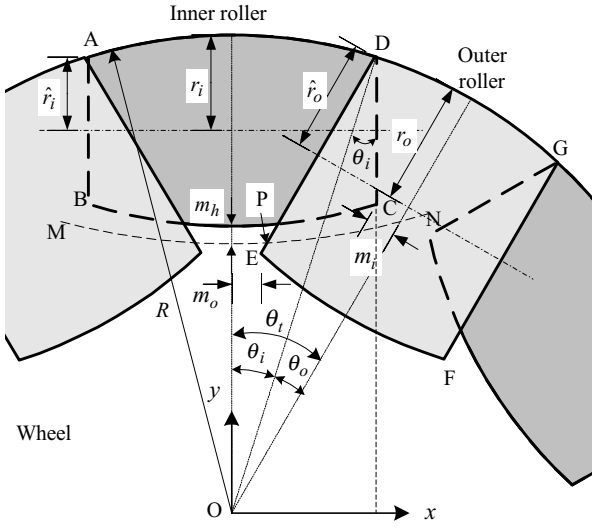

Fig. 2 Alternate inner and outer rollers

The height of a surmountable bump for a universal wheel with passive rollers depends on the size of the minimum radius (not on the wheel radius) and friction of a roller [6]. Therefore, it is preferable that the minimum radius of a roller be as large as possible and thus approach the maximum radius for a given wheel size. In this regard, the half wheel structure is not desirable because the minimum radius is small compared with the maximum one.

2.1 Number and radii of rollers

Fig. 2 shows the configuration of a continuous alternate wheel where the inner and outer rollers are alternated. As mentioned previously, since virtually no gap between rollers exists, the wheel contacts the ground continuously. First the conditions for no gap between rollers will be investigated below.

From the geometry in Fig. 2, the relationship between the wheel radius R and the half-angles θ_i and θ_o for the inner and outer rollers, respectively, becomes

$$2n(\theta_i + \theta_o) = 2\pi \tag{1}$$

where n represents the number of inner (or outer) rollers. If n = 4, for example, the wheel consists of 4 inner rollers and 4 outer rollers, and thus θ_t ($=\theta_i+\theta_o$) becomes $\pi/4$. The maximum radius r_i and the minimum radius $\hat{r}_i$ of an inner roller have the geometric relation

$$(R - r_i + \hat{r}_i)^2 + R^2 \sin^2\theta_i = R^2 \tag{2}$$

and the maximum radius r_o and the minimum radius $\hat{r}_o$ of an outer roller have the similar relation

$$(R - r_o + \hat{r}_o)^2 + R^2 \sin^2\theta_o = R^2 . \tag{3}$$

Next, for no overlapping of inner rollers, the minimum radius of a inner roller should satisfy the following condition

$$(R\sin\theta_o - m_i) \geq 2\hat{r}_i \sin(\theta_i + \theta_o) \tag{4}$$

where m_i is the space margin between the inner rollers, which depends on the size of the supporting frame (refer to Section 3). The minimum radius of an inner roller is then obtained by

$$\hat{r}_i \leq \frac{R\sin\theta_o - m_i}{2\sin(\theta_i + \theta_o)} \tag{5}$$

and thus the upper limit on $\hat{r}_i$ becomes

$$\hat{r}_{i\max} = \frac{R\sin\theta_o - m_i}{2\sin(\theta_i + \theta_o)} . \tag{6}$$

Then the upper limit on r_i is easily computed by

$$r_{i\max} = \hat{r}_{i\max} + R(1 - \cos\theta_i) . \tag{7}$$

Similarly, the condition for no overlapping of outer rollers on the minimum radius of the outer roller is obtained by

$$\hat{r}_o \leq \frac{R\sin\theta_i - m_o}{2\sin(\theta_i + \theta_o)} \tag{8}$$

where m_o represents the margin between the outer rollers, which depends on the size of the supporting frame. The upper limits on the minimum and maximum radii of the outer rollers are given by

$$\hat{r}_{o\max} = \frac{R\sin\theta_i - m_o}{2\sin(\theta_i + \theta_o)} , \tag{9}$$

$$r_{o\max} = \hat{r}_{o\max} + R(1 - \cos\theta_o) . \tag{10}$$

The next step is to find the geometric conditions that the inner and outer rollers do not overlap. Since the rollers are solid as shown in Fig. 2, some portion of the inner roller interpenetrates inside of the outer roller. This problem will discussed in Section 2.2, and the condition to avoid overlap between surfaces of the inner and outer rollers is first considered here. Let the xy coordinates be defined at the center of the wheel as shown in Fig. 2. The

equation for segment DE is given by

$$y = \frac{1}{\tan(\theta_i + \theta_o)}(x - R\sin\theta_i) + R\cos\theta_i \tag{11}$$

and the equation of the circle offset by the margin m_h from the surface of the inner roller (represented by the dashed arc MN) is described by

$$x^2 + \{y - (2R - 2r_i - m_h)\}^2 = R^2 \tag{12}$$

Solving Eq. (11) and (12) yields the intersecting point P whose coordinates are

$$x_P = \frac{-ae \pm \sqrt{a^2 - e^2 + 1}}{a^2 + 1}, \tag{13a}$$

$$y_P = a(x_P - b) + c \tag{13b}$$

where $a = 1/\tan(\theta_i + \theta_o)$, $b = R\sin\theta_i$, $c = R\cos\theta_i$,
$d = 2R - 2r_i - m_h$, $e = -ab + c - d$.

To avoid overlap, the segment DP must be less than or equal to the minimum diameter DE of the outer roller. Hence

$$\hat{r}_{o\min} = \frac{\sqrt{(R\sin\theta_i - x_P)^2 + (R\cos\theta_i - y_P)^2}}{2} \tag{14a}$$

The lower limit on the maximum radius of the outer roller then becomes

$$r_{o\min} = \hat{r}_{o\min} + R(1 - \cos\theta_o) \tag{14b}$$

In summary, given a wheel radius R and the margins m_i, m_o, m_h, the upper and lower limits for radii of the inner and outer rollers can be determined as a function of θ_i (or equivalently θ_o) and n. For example, when m_i, m_o, m_h are set to 5.5mm, 4.5mm, 7.0mm, respectively, for a wheel radius of 10cm, the roller radii as a function of θ_i for n in the range of 3 to 8 are illustrated in Fig. 3. In Fig. 3, the maximum radius of an outer roller should be searched for in the region of $r_{o\max} \geq r_{o\min}$; otherwise, no solution exists. It is found that there is no solution for $n = 3$, since $r_{o\min}$ is greater than $r_{o\max}$ in the entire range of θ_i. Since the height of a surmountable bump is limited by the minimum radius of the inner roller, which is the smallest among four different radii, the roller shape should be decided so that the minimum radius of an inner roller has the largest value. It is observed in Fig. 3 that as θ_i increases, the radii of the outer roller increase, but those of the inner roller decrease. Therefore, the largest minimum radius of the inner roller corresponds to the point where $r_{o\max} = r_{o\min}$ in the plots. By equating Eq. (10) and (14b), the following equation is obtained.

$$\frac{\sqrt{(R\sin\theta_i - x_P)^2 + (R\cos\theta_i - y_P)^2}}{2} = \frac{R\sin\theta_i - m_o}{2\sin(\theta_i + \theta_o)} \tag{15}$$

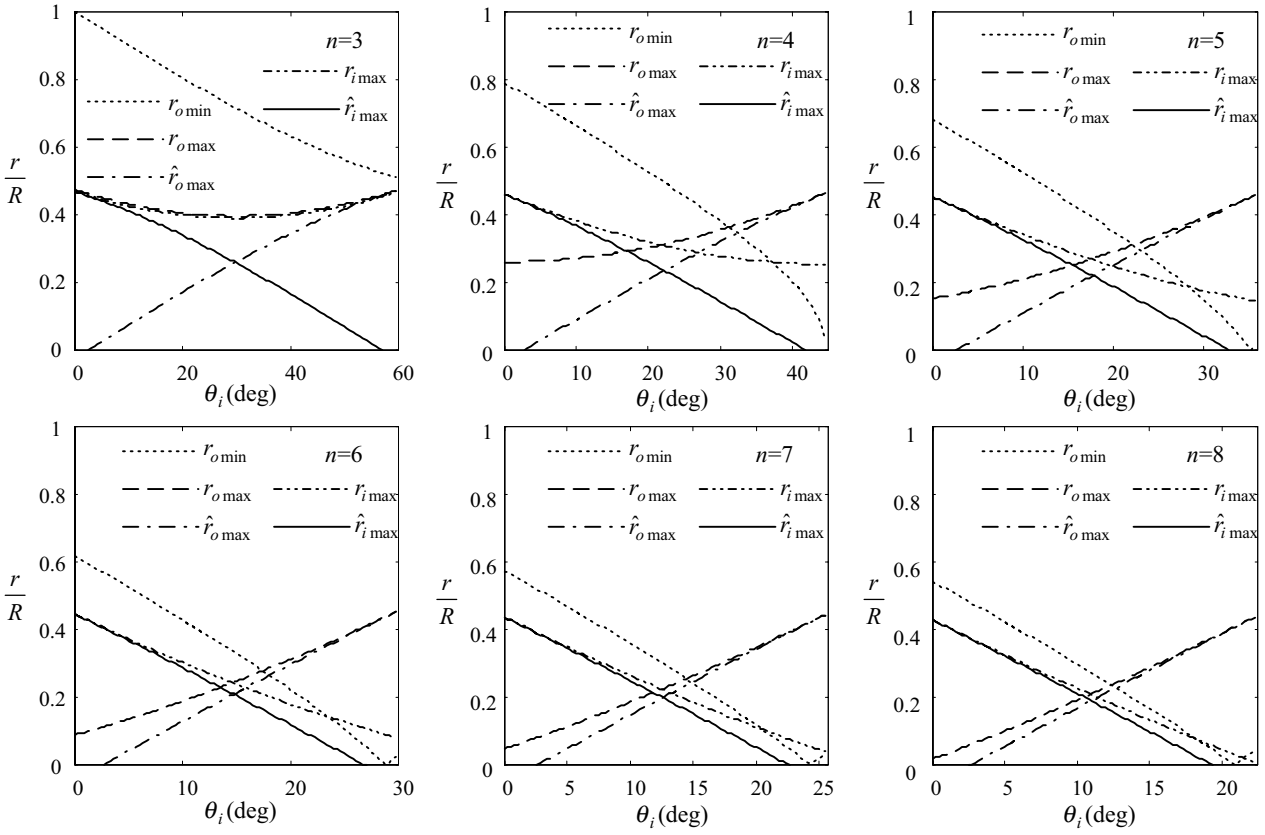

Fig. 3 Roller radii as a function of θ_i for various values of n

Since this equation cannot be solved explicitly, the solution by a numerical analysis technique should be obtained. Fig. 4 shows computational results of the roller radii as a function of n.

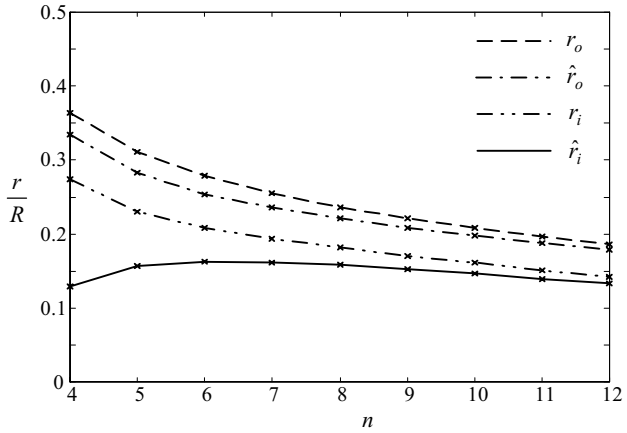

Fig. 4 Variation of radii of inner and outer rollers as a function of n

It is noted from Fig. 4 that for $n < 6$, the minimum radius of an inner roller becomes smaller while the other radii get larger. For $n > 6$, all the radii tend to decrease, which is not desirable. Considering all these facts, the number of rollers was chosen as 6 in the example design of a continuous alternate wheel.

2.2 Shape of inside of outer roller

Since the structure of the continuous alternate wheel involves slight interpenetration of the inner roller into the interior of the outer roller, the inside surface of the outer roller must have some inclination (denoted DH in Fig. 5) to avoid interference with the side surface (whose diameter is CD) of the inner roller. As the angle ϕ between the x axis and DH decreases, the inside surface of an outer roller can be thicker, thus leading to more solid structure.

The side circle of an inner roller whose diameter is CD can be found by the intersection of the sphere and the plane represented by

$$(x-\hat{r}_i\cos\theta_t)^2+(y-\hat{r}_i\sin\theta_t)^2+z^2=\hat{r}_i^2, \tag{16}$$

$$y=\tan\theta_t x. \tag{17}$$

Combining Eq. (16) and (17) gives the following equation of circle

$$\left(\frac{x}{\cos\theta_t}-\hat{r}_i\right)^2+z^2=\hat{r}_i^2 \quad , \quad y=\tan\theta_t x. \tag{18}$$

The distance L between this circle and the axis (represented by the segment PH) that passes the point $(\hat{r}_o,0,0)$ and is parallel to the y-axis is expressed by

$$L^2=(x-\hat{r}_o)^2+z^2. \tag{19}$$

Substituting Eq. (17) and (18) into (19) yields

$$L(y)^2=-y^2-2\left(\frac{\hat{r}_o\cos\theta_t-\hat{r}_i}{\sin\theta_t}\right)y+\hat{r}_o^2 \tag{20a}$$

or, equivalently,

$$L(y)=\pm\sqrt{\hat{r}_o^2-y^2-2\left(\frac{\hat{r}_o\cos\theta_t-\hat{r}_i}{\sin\theta_t}\right)y}\,. \tag{20b}$$

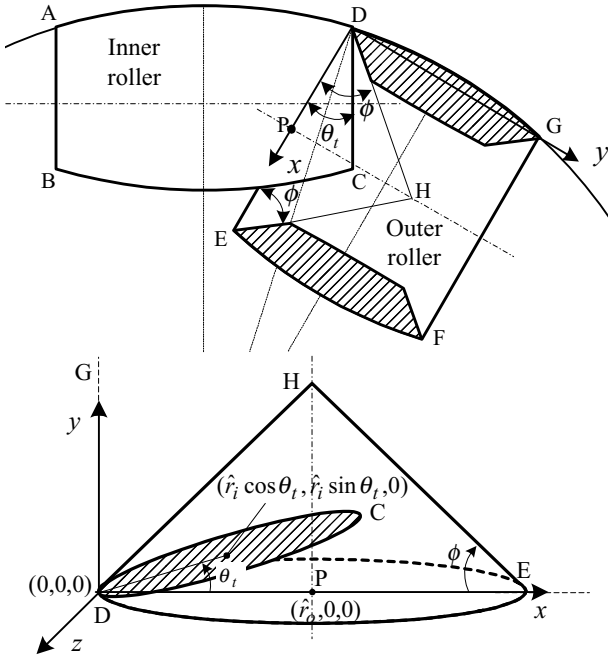

Fig. 5 Interpenetration of inner roller into outer roller

Partial differentiation of Eq. (20b) with respect to y gives

$$\frac{\partial L(y)}{\partial y}=-\frac{y+\dfrac{\hat{r}_o\cos\theta_t-\hat{r}_i}{\sin\theta_t}}{\sqrt{\hat{r}_o^2-y^2-2\left(\dfrac{\hat{r}_o\cos\theta_t-\hat{r}_i}{\sin\theta_t}\right)y}}. \tag{21}$$

From Eq. (21), the minimum angle ϕ to avoid interference can be found at $y = 0$

$$\frac{\partial L(0)}{\partial y}=-\frac{1}{\hat{r}_o}\frac{\hat{r}_o\cos\theta_t-\hat{r}_i}{\sin\theta_t}=\frac{\hat{r}_i/\hat{r}_o-\cos\theta_t}{\sin\theta_t}. \tag{22}$$

Table 1 shows the results of computation for a given example. Since the number of rollers was chosen as 6, the total roller angle becomes 30°, and θ_i is determined to be 17.4°.

Table 1 Design parameters for continuous alternate wheel

n	6	r_o	27.8mm
R	10cm	$\hat{r}_o$	25.4mm
θ_i	17.4°	r_i	20.9mm
θ_o	12.6°	$\hat{r}_i$	16.3mm
ϕ	24.3°		

3. Structure of continuous alternate wheel

An actual continuous alternate wheel was fabricated based on the design parameters given in Table 1. In the process of fabrication, more design factors other than the previously determined ones such as the number of rollers, roller radii, the inside inclination angle of an outer roller were considered. This section is concerned with the overall structure of a continuous alternate wheel.

3.1 Rollers

The shapes of inner and outer rollers designed in the previous section are capable of continuously contacting the ground without any interference between rollers.

Polyurethane was selected as the roller material since it provides a friction coefficient and mechanical properties suited to a universal wheel. However, a urethane roller is not solid enough to prevent deformation when it is subject to loads due to contact with the ground. Therefore, supporting frames in the form of a hollow cylinder are inserted inside the rollers to support urethane rollers.

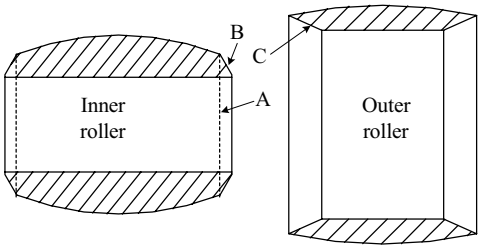

Fig. 6 Final shapes of rollers

Referring to Fig. 5, the fringe of the outer roller is relatively thin to avoid interference with the inner roller. However, this thin part cannot be supported by any supporting frame, since it interferes with the inner roller. As a result, this thin fringe of the outer roller is not solid enough to bear the external load due to contact with the ground. To overcome this problem, the final shapes of the rollers are designed as shown in Fig. 6. The inside surface of an outer roller forms a circular cone (denoted C in Fig. 6) with the inclination angle determined by the previous analysis. Note that another circular cone (denoted B) is added to the original sides of the inner roller (denoted A). These circular cones B and C do not contact each other when they are not subject to a load, since a small margin exists between the two surfaces. When the thin part of the outer roller makes contact with the ground, however, surface C is pressed against surface B. Then, surface B support surface C, and actually they rotate together about each roller axis. In this way, the problem of deformation of the fringe of the outer roller can be overcome without causing any interference with the inner roller.

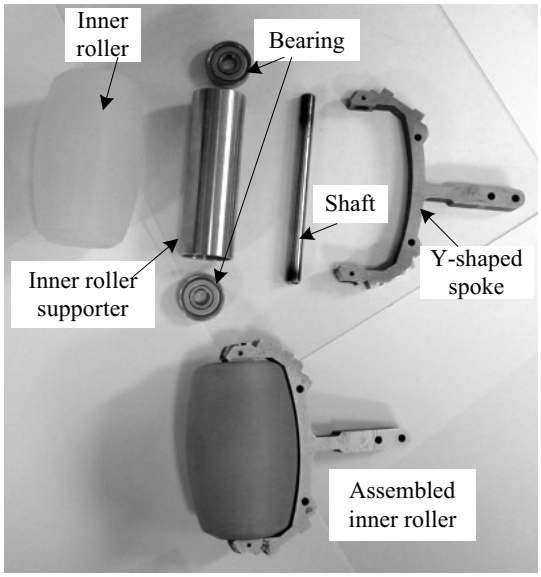

(a) Parts of inner roller

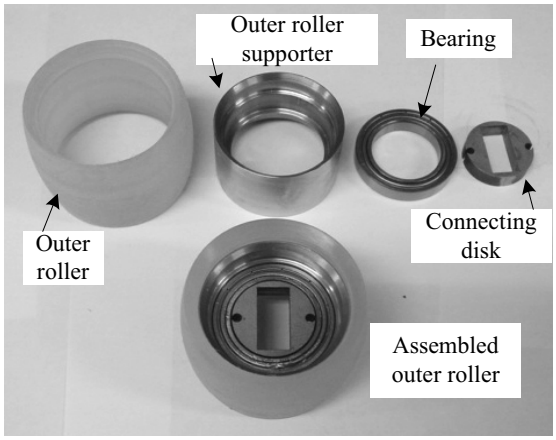

(b) Parts of outer roller

Fig. 7 Photo of roller parts and assembled rollers

3.2 Supporting structure

A supporting structure is required to place rollers around the wheel. The supporting structure for the inner roller is composed of a supporter, a spoke, a roller axis and bearings, while that for the outer roller consists of a supporter and bearings as shown in Fig. 7. One reason why other universal wheels have a gap between rollers is the space for the supporting structure. In the proposed wheel, however, no gap is required since the outer roller was designed to enclose the supporting structure and part of the inner rollers.

Fig. 8 shows schematic diagram and cutaway view of the final wheel and Fig. 9 is a photo of the continuous alternate wheel. As shown in Fig. 8, the wheel has a hub with radially disposed six Y-shaped spokes made of stainless steel. Each spoke supports one inner roller through the roller axis with bearings at both ends. Two consecutive spokes, on the other hand, support the outer roller together through bearings. Note that the margins m_i, m_o, and m_h were considered at the beginning of the design

to provide appropriate space for spokes.

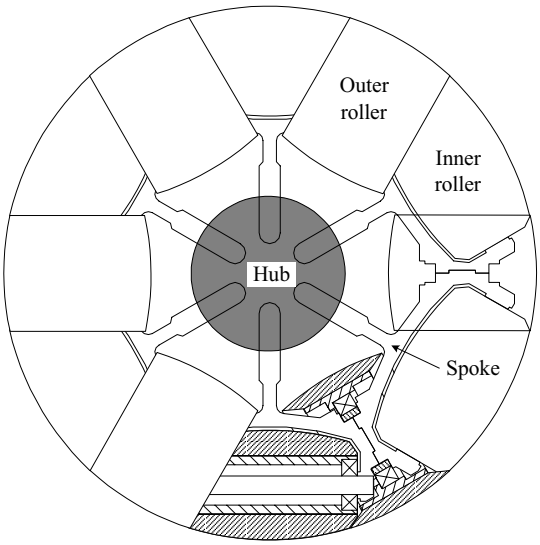

Fig. 8 Schematic diagram of continuous alternate wheel

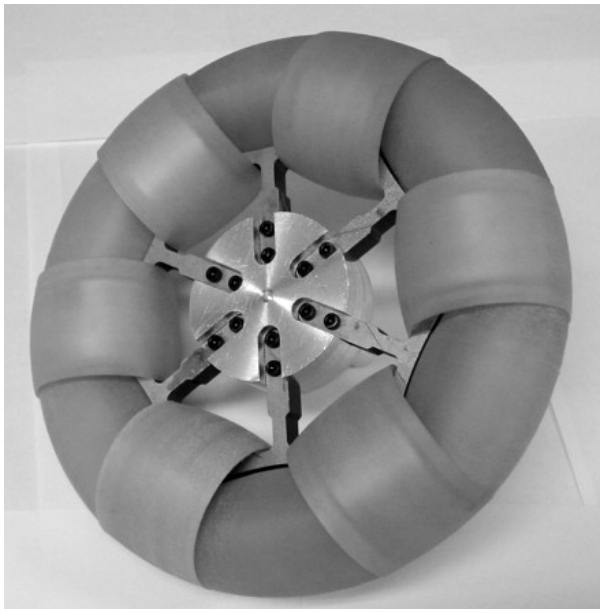

Fig. 9 Photo of continuous alternate wheel

4. Conclusion

In this research a novel design of continuous alternate wheel was proposed to minimize a gap between rollers, which causes vertical and/or horizontal vibrations in many types of omni-directional wheels with passive rollers. This wheel is an improved version of a conventional alternate wheel where inner and outer rollers are disposed alternately. In the continuous alternate wheel, however, the inner and outer rollers are arranged continuously, thus resulting in no gap between the rollers.

This paper details the design process of the continuous alternate wheel. The systematic approaches were presented to determine the optimum number of rollers, the radii of rollers, and the inclination angle of the inside of an outer roller for given design specifications

Using the polyurethane rollers, the actual continuous alternate wheel was constructed to verify validity of the design guidelines. The omnidirectional mobile robots equipped with these proposed wheels are now under construction.

References

[1] Wada, M, Mory, S, "Holonomic and omnidirectional vehicle with conventional tires," 1996 *Int. Conf. On Robotics and Automation*, pp.3671-3676, 1996.

[2] West, M., Asada, H., "Design of ball wheel mechanisms for omnidirectional vehicles with full mobility and invariant kinematics," *Journal of mechanical design*, pp.119-161, 1997.

[3] Blumrich, J. F., "Omnidirectional vehicle," *United States Patent* 3,789,947, 1974.

[4] Ilou, B. E., "Wheels for a course stable self-propelling vehicle movable in any desired direction on the ground or some other base," *United States Patent* 3,876,255, 1975.

[5] Asada, H, Sato, M, Bogoni, L, "Holonomic and omnidirectional vehicle with conventional tires," 1995 *Int. Conf. On Robotics and Automation*, pp.1925-1930, 1995.

[6] Ferriere, L., Raucent, B., and Campion, G., "Design of omnimobile robot wheels," 1996 *Int. Conf. On Robotics and Automation*, pp.3664-3670, 1996.

[7] Carlisle, B., "An omni-directional mobile robot," *Development in robotics*, Kempston, pp. 79-87, 1983.